Range-Doppler Ambiguity Mitigation via Closed-Loop, Adaptive PRF Selection

C. M. Kenyon[1] N. A. Goodman[2]

Abstract - **In this paper, we present a method of calculating and updating target probabilities in ambiguous range-Doppler cells along with an adaptive pulse repetition frequency (PRF) selection technique based on mutual information (MI). We approach the problem of updating the probability in multiple ambiguous cells by using a multiple hypothesis test for the target state. The probability ensemble is then used to determine which PRF will maximize MI on the next update. Since MI is a measure of the reduction in entropy of the ensemble, it indicates the amount of information the radar stands to learn about the channel due to the selected PRF. We compare the results of MI-based PRF selection to two other PRF selection methods and demonstrate how blind zones and clutter aliasing can be seamlessly integrated into our PRF-selection procedure.**

1 INTRODUCTION

Range-Doppler ambiguities are well-known phenomena of pulsed radar systems that limit performance. These ambiguities are caused by aliasing in the time and frequency domains and their structure is controlled by pulse repetition frequency (PRF). Coding of individual pulses and using waveforms with varying PRF (also known as staggered PRF) have been suggested to solve this problem [1-3]. These methods are designed to work well in traditional radar systems where decisions about target states are uninfluenced by previous measurements and data are only valid for a single collection interval.

Cognitive radar (CR) interprets the propagation channel as a random ensemble of potential target states [4]. In contrast to classical radar, CR retains information from past measurements in a probability map describing target parameters such as range and Doppler. CR gains a probabilistic understanding of the channel using adaptive probing methods.

In this paper, we present a PRF selection technique based on maximizing mutual information between radar measurements and a probabilistic representation of the range-Doppler space. In Section 2, we describe the scenario model. Section 3 describes our multiple hypothesis framework and our probability update. The mutual-information-based PRF selection criterion is explained in Section 4. We show results in Section 5. Concluding remarks are presented in Section 6.

2 SCENARIO MODEL

We focus our discussion on pulsed monostatic radar systems. The propagation channel consists of point targets, random noise, and clutter from unwanted ground returns. Let m denote the range-Doppler cell from which a signal is received. The range measurement (fast-time) indices are $n = 0,1,\dots,N-1$ and the Doppler measurement (slow-time) indices are $l = 0,1,\dots L-1$. For a radar system, the range and Doppler states of a target can be interpreted as frequencies. Let the normalized range and Doppler frequencies for a target in the m^{th} bin be f_{R_m} and f_{D_m}, respectively. Only cells with different frequencies can be resolved. The received signal produced by a target in the m^{th} cell is proportional to a normalized fast-time/slow-time steering vector given by

$$\boldsymbol{s}_m = \frac{1}{\sqrt{L\cdot N}}\exp\left(-j2\pi f_{R_m}[0\dots n\dots N-1]^T\right)\otimes \exp\left(-j2\pi f_{D_m}[0\dots l\dots L-1]^T\right). \quad (1)$$

Equation (1) illustrates that aliasing occurs when range and/or Doppler normalized frequencies differ by an integer amount. Cells with aliased frequencies are indistinguishable (ambiguous). Range ambiguities are controlled by PRF according to

$$R_{a,max} = \frac{c}{2\cdot PRF} \quad (2)$$

where c is the speed of light and the factor of two in the denominator accounts for the roundtrip. The maximum unambiguous Doppler is directly related to PRF according to

$$F_{d,max} = PRF. \quad (3)$$

Equations (2) and (3) show the well-known inverse relationship between range and Doppler ambiguities.

Since transmitter and receiver are collocated in a monostatic radar, the receiver must turn off during pulse transmission to protect the hardware from damage. This causes unobservable ranges known as blind zones which are described by

$$R_{blind} = \frac{c\cdot t_p}{2} \quad (4)$$

where t_p is the width of the pulse in seconds.

We form a two-dimensional grid of possible range and Doppler values. Associated with each range-Doppler bin in the grid is a probability that a target is present in that bin. Different permutations of target presence/absence in various bins forms the ensemble of potential target states. For simplicity, we assume the grid is square with M range and M Doppler bins where M is larger than the number of unambiguous bins in either dimension. The channel is described by a set of M^2 probabilities.

[1] Department of Electrical and Computer Engineering, University of Arizona, Tucson Arizona, 85721, USA
e-mail: ckenyon@email.arizona.edu
[2] Department of Electrical and Computer Engineering, University of Arizona, Tucson Arizona, 85721, USA
e-mail: goodman@ece.arizona.edu

978-1-4244-7368-7/10/$26.00 ©2010 IEEE

Let J be the number of distinct PRFs available to the radar and N_j be the number of range-Doppler ambiguities when the j^{th} PRF is used. Figure 1 is a rendering of the ensemble with the first group of ambiguous cells shaded.

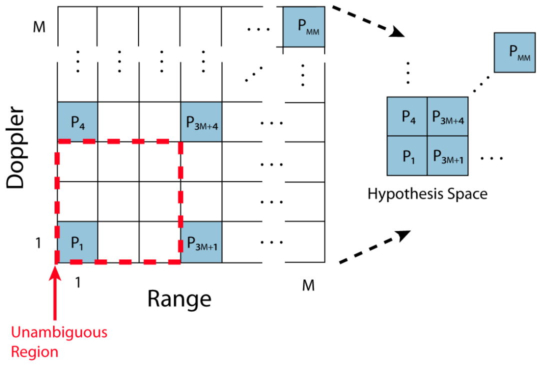

Figure 1: Illustration of ensemble and formation of hypothesis space. Shaded cells are ambiguous.

The presence/absence of a target in any cell is independent of target presence/absence in other cells. A multiple hypothesis framework can be used to describe the 2^{M^2} number of possible target states. Each hypothesis may be thought of as a joint hypothesis corresponding to a unique permutation of target presence/absence in individual cells. The target hypotheses are

$$\begin{aligned} &H_0: \boldsymbol{z} = \boldsymbol{n} + \boldsymbol{c}_0 \\ &H_1: \boldsymbol{z} = \alpha_1 \boldsymbol{s}_1 + \boldsymbol{n} + \boldsymbol{c}_1 \\ &H_2: \boldsymbol{z} = \alpha_2 \boldsymbol{s}_2 + \boldsymbol{n} + \boldsymbol{c}_2 \\ &\vdots \\ &H_{2^{M^2}-1}: \boldsymbol{z} = \alpha_1 \boldsymbol{s}_1 + \alpha_2 \boldsymbol{s}_2 + \cdots \alpha_m \boldsymbol{s}_m \\ &\qquad + \cdots \alpha_{M^2} \boldsymbol{s}_{M^2} + n + \boldsymbol{c}_{2^{M^2}-1} \end{aligned} \tag{5}$$

where the reflection coefficient α_m is modeled as a random variable with Rayleigh distributed amplitude and uniformly distributed phase. The noise, $\boldsymbol{n}$, is a complex Gaussian random vector with zero mean and covariance matrix $\sigma_n^2 \boldsymbol{I}$. The clutter, $\boldsymbol{c}$, is distributed according to $CN(\boldsymbol{0}, \boldsymbol{R}_c)$. We assume the radar platform is stationary which centers the clutter at zero Doppler. We also assume the clutter is uncorrelated in range and model the clutter as having a power spectral density (PSD) in the shape of a hanning window.

3 PROBABILITY UPDATE

For cells that are resolvable and unambiguous, target probabilities can be updated separately in each cell based on an observed CPI. However, the probabilities of ambiguous cells cannot be updated separately and must be treated jointly. Using the hypotheses described in the previous section, a set of ambiguous joint hypotheses can be obtained for every uniquely resolvable range-Doppler cell (see Figure 1). In this section, we first show the general probability update procedure, then show the special case of resolvable cells.

3.1 Procedure for the General Case

The *pdf* for the measured data under the i^{th} joint hypothesis from (5) is

$$p(\boldsymbol{z}|H_i) = \frac{1}{\pi^N \left|\boldsymbol{R}_{s_i} + \sigma_n^2 \boldsymbol{I} + \boldsymbol{R}_{c_i}\right|^N} \cdot \exp\left[-\boldsymbol{z}^H (\boldsymbol{R}_{s_i} + \sigma_n^2 \boldsymbol{I} + \boldsymbol{R}_{c_i})^{-1} \boldsymbol{z}\right] \tag{6}$$

where $\boldsymbol{R}_{s_i}$ and $\boldsymbol{R}_{c_i}$ are the target and the clutter covariance matrices, respectively, for the measurement under the i^{th} hypothesis.

Our goal is to update the individual cell probabilities. We must first update the joint hypotheses using Bayes' rule, which gives the posterior probability for a single joint hypothesis as

$$P(H_i|\boldsymbol{z}_k) = \frac{P(H_i|\boldsymbol{z}_{k-1}) p(\boldsymbol{z}_k|H_i)}{p(\boldsymbol{z}_k)} \tag{7}$$

where $P(H_i|\boldsymbol{z}_k)$ is the probability of hypothesis i after collecting k CPIs. The denominator of (7) may not be readily available, however it is the same for all joint hypotheses and can be replaced by a factor β which normalizes the sum of the joint hypotheses yielding

$$P(H_i|\boldsymbol{z}_k) = \beta P(H_i|\boldsymbol{z}_{k-1}) p(\boldsymbol{z}_k|H_i). \tag{8}$$

We now describe how to obtain $P(H_i|\boldsymbol{z}_{k-1})$, the probability of the i^{th} hypothesis prior to the k^{th} CPI. The probability of a joint hypothesis can be calculated by multiplying the probabilities of the individual cells in that hypothesis according to

$$\begin{aligned} &P(H_0|\boldsymbol{z}_{k-1}) = \overline{P_1 P_2 P_3} \ldots \overline{P_{MM}} \\ &P(H_1|\boldsymbol{z}_{k-1}) = P_1 \overline{P_2 P_3} \ldots \overline{P_{MM}} \\ &P(H_2|\boldsymbol{z}_{k-1}) = \overline{P_1} P_2 \overline{P_3} \ldots \overline{P_{MM}} \\ &\vdots \\ &P(H_{2^{M^2}-1}|\boldsymbol{z}_{k-1}) = P_1 P_2 P_3 \ldots P_{MM} \end{aligned} \tag{9}$$

where the overbar represents $(1 - P_m)$. Thus, (9) describes how to obtain prior probabilities for a joint hypothesis and (6) gives the data *pdf* for a joint hypothesis. These are used to update as in (8), then the updated joint hypothesis probabilities are converted back to cell probabilities by finding the marginal probabilities from $P(H_i|\boldsymbol{z}_k)$.

3.2 Procedure for the Resolvable Cell Case

As mentioned earlier, resolvable cells can be treated separately. While the multiple hypothesis framework presented in (5) is valid for this case, it is computationally more efficient to perform separate probability updates for resolvable cells. For the m^{th} cell, let $\mathcal{H}_{m,0}$ and $\mathcal{H}_{m,1}$ be the target null and present hypotheses. Bayes' rule for an individual cell probability is then

$$P(\mathcal{H}_{m,0}|\mathbf{z}_k) = \frac{P(\mathcal{H}_{m,0}|\mathbf{z}_{k-1})p(\mathbf{z}_k|\mathcal{H}_{m,0})}{p(\mathbf{z}_k)} = \gamma P(\mathcal{H}_{m,0}|\mathbf{z}_{k-1})p(\mathbf{z}_k|\mathcal{H}_{m,0}) \quad (10)$$

$$P(\mathcal{H}_{m,1}|\mathbf{z}_k) = \frac{P(\mathcal{H}_{m,1}|z_{k-1})p(\mathbf{z}_k|\mathcal{H}_{m,1})}{p(\mathbf{z}_k)} = \gamma P(\mathcal{H}_{m,1}|\mathbf{z}_{k-1})p(\mathbf{z}_k|\mathcal{H}_{m,1}). \quad (11)$$

For Q resolvable range-Doppler cells, the update procedure can be divided into Q separate update calculations, one for each ambiguity group. Each calculation has N_q joint hypotheses where index q represents the ambiguity group being considered.

4 MUTUAL-INFORMATION-BASED PRF SELECTION

4.1 Closed-Loop Operation

Our goal is to detect targets in range and Doppler using the probabilities calculated in the previous section. We can represent target presence/absence in the m^{th} cell as a binary random variable x_m. Unfortunately, there is no closed-form for the mutual information $I(\mathbf{z}_k; x_m)$ since x_m is a binary random variable and $\mathbf{z}_k$ is a Gaussian mixture. A technique for estimating the mutual information $I(\mathbf{z}_k; x_m)$ based on a quantity known as *spectral variance* is presented in [5]. In order to show how the principles in [5] apply to our case, we define a new mutual information calculation $I(\mathbf{z}_k; \widetilde{\mathbf{x}}_q)$ where $\widetilde{\mathbf{x}}_q$ is a binary random vector for the q^{th} group of ambiguous cells. For the case in Figure 1, $\widetilde{\mathbf{x}}_1$ is

$$\widetilde{\mathbf{x}}_1 = [\tilde{x}_1 \ \tilde{x}_4 \dots \tilde{x}_{3M+1} \ \tilde{x}_{3M+4} \dots \ \tilde{x}_{MM}]. \quad (12)$$

Binary random variables $\tilde{x}_m$ representing target presence/absence in the m^{th} cell form the elements of $\widetilde{\mathbf{x}}_q$. Let the mutual information for one group of ambiguous cells be defined as

$$I(\mathbf{z}_k; \widetilde{\mathbf{x}}_q) = \log(1 + \widehat{SNR}_q) \quad (13)$$

where

$$\widehat{SNR}_q = \frac{\widehat{\sigma^2}_{s,q}}{\sigma_n^2 + \sigma_c^2}. \quad (14)$$

Equation (13) approximates the information the radar stands to learn about the propagation channel in bits. The joint hypotheses are used to obtain $\widehat{\sigma^2}_{s,q}$, an estimate of the target variance for the q^{th} ambiguity group. This is similar to how a spectral variance from [5] is used to design matched-illumination waveforms in [6, 7]. Using the probabilities of the joint hypotheses from the q^{th} ambiguity group, the estimated target variance is

$$\widehat{\sigma^2}_{s,q} = \sum_{i=0}^{N_q-1} P_i \sigma_i^2 - \left| \sum_{i=0}^{N_q-1} P_i \sigma_i \right|^2 \quad (15)$$

where σ_i^2 is the RCS for the i^{th} joint hypothesis. This process is repeated for all Q groups of ambiguous cells in the ensemble. The total mutual information of the ensemble for one PRF is

$$I(\mathbf{z}_k; \widetilde{\mathbf{x}}) = \sum_{q=1}^{Q} I(\mathbf{z}_k; \widetilde{\mathbf{x}}_q). \quad (16)$$

The PRF that maximizes mutual information in (16) is chosen to produce the waveform for the next CPI.

4.2 Termination Criterion: Binary Hypothesis Test

In this subsection, we present a binary hypothesis test introduced by Wald [8] to determine when our adaptive PRF system should cease waveform transmission.

We only need to decide if a target is present or absent in each cell. The probability that a target is present in the m^{th} cell is P_m. Let Λ_m^k be a decision statistic for the m^{th} cell calculated after the k^{th} transmission given by

$$\Lambda_m^k = \frac{p_{01}(z_1)p_{02}(z_2)\cdots p_{0k}(z_k)}{p_{11}(z_1)p_{12}(z_2)\cdots p_{1k}(z_k)} \frac{1 - P_\mathrm{m}}{P_\mathrm{m}}. \quad (17)$$

Lowercase $p_{ik}(\mathbf{z}_k)$ is the *pdf* of the measurement at the k^{th} iteration, $\mathbf{z}_k$. The first subscript on p represents the hypothesis under test, target present or target absent. Let α represent the probability of declaring a target when no target is present. After each transmission, we compute

$$\Lambda_m^k > \frac{1 - \alpha_m}{\alpha_m} \quad (18)$$

for all cells in the ensemble. If all cells pass the criterion defined in (18), the target probabilities are close to 0 or 1 and the algorithm terminates.

4.3 Exceptions

Due to constraints of radar systems, a blind zone always exists close to the radar. The probabilities in the blind cells never get updated. Thus the termination criterion is not applied to these cells.

5 SIMULATION RESULTS

Results for mutual information, random, and coprime PRF selection schemes are presented in this section. The results are obtained from a 160-run Monte Carlo simulation. Clutter is present in all cases and has a clutter-to-noise ratio (CNR) of 40 dB per measurement. For the MI and random-PRF selection cases, the radar was allowed to choose from four PRFs. Two coprime PRFs alternated between CPIs for the coprime scenario. For the results shown in this section, all cells in the ensembles were initialized to a probability of 0.05. The PRF of the first CPI was randomly chosen from the available PRFs.

Figure 2 shows the average number of CPIs required for each algorithm to meet the termination criterion. The amount of target information per CPI increases with increasing SNR; therefore, it is expected that the number of scans required to meet the termination criterion decreases as SNR increases. The MI selection scheme exhibits better performance than the other two cases because it maximizes the information obtained from the radar channel in each scan.

Figure 3 shows the average mutual information per CPI vs SNR per CPI. Mutual information is a measure of the decrease in uncertainty of the ensemble. As SNR per CPI increases, more information can be extracted from the channel in each CPI. Therefore, the mutual information increases with increasing SNR as expected. Figure 3 can be interpreted as showing the mutual information per unit energy.

The final metric we show to assess the MI algorithm is probability of detection (P_D) per CPI or, equivalently, per unit energy. This is shown in Figure 4. The MI algorithm illustrated a marked improvement in P_D over the random and coprime techniques.

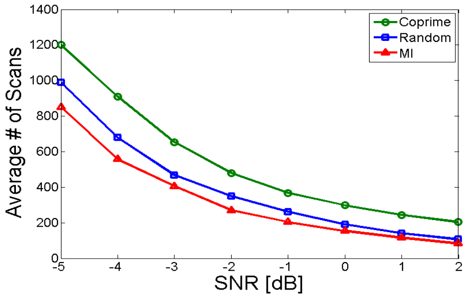

Figure 2: Comparison of number of transmissions required to reach termination criterion

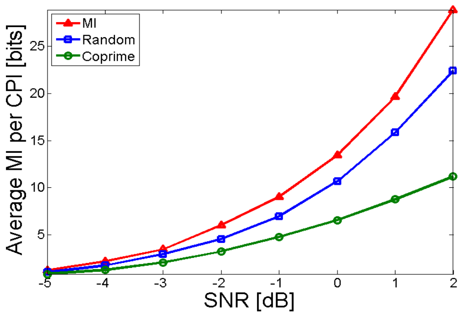

Figure 3: Comparison of average mutual information per unit energy transmitted

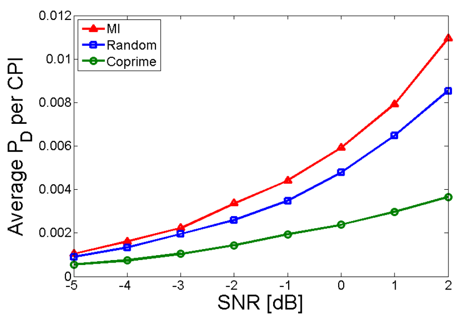

Figure 4: Comparison of probability of detection per unit energy transmitted

6 CONCLUSION

In this paper, we developed a PRF selection technique based on maximum mutual information and described how to obtain and update target probabilities for ambiguous range-Doppler cells using a set of joint hypotheses. We described the difficulty in determining the actual state of the binary random variable that describes target presence/absence in the ensemble cells and presented a technique used in [5-7] to estimate spectral variance of the ensemble. Finally, we presented results showing the mutual information PRF selection technique is superior to a random PRF selection technique and a scheme that alternates between two coprime PRFs.

References

[1] J. M. Anderson, M. A. Temple and M. E. Oxley, "Nonlinear suppression of range ambiguities in pulse-diverse radar," *Electronics Letters,* vol. 37, pp. 1252-1253, 2001.

[2] J. J. Benedetto, I. Konstantinidis and M. Rangaswamy, "Phase-Coded Waveforms and Their Design," *Signal Processing Magazine, IEEE,* vol. 26; 26, pp. 22-31, 2009.

[3] N. Reddy and M. Swamy, "Resolution of range and Doppler ambiguities in medium PRF radars in multiple-target environment," *Acoustics, Speech, and Signal Processing, IEEE International Conference on ICASSP '84.,* vol. 9; 9, pp. 514-517, 1984.

[4] S. Haykin, "Cognitive radar: a way of the future," *Signal Processing Magazine, IEEE,* vol. 23, pp. 30-40, 2006.

[5] M. R. Bell, "Information theory and radar waveform design," *Information Theory, IEEE Transactions on,* vol. 39; 39, pp. 1578-1597, 1993.

[6] N. A. Goodman, P. R. Venkata and M. A. Neifeld, "Adaptive Waveform Design and Sequential Hypothesis Testing for Target Recognition With Active Sensors," *Selected Topics in Signal Processing, IEEE Journal of,* vol. 1; 1, pp. 105-113, 2007.

[7] P. Nielsen and N. A. Goodman, "Integrated detection and tracking via closed-loop radar with spatial-domain matched illumination," *Radar, 2008 International Conference on,* pp. 546-551, 2008.

[8] A. Wald, "Sequential analysis," New York: Wiley, 1947.